The Aftershock Signature of Supershear Earthquakes

Michel Bouchon, *et al.*

Science **320**, 1323 (2008);
DOI: 10.1126/science.1155030

The Aftershock Signature of Supershear Earthquakes

Michel Bouchon[1]* and Hayrullah Karabulut[2]

Recent studies show that earthquake faults may rupture at speeds exceeding the shear wave velocity of rocks. This supershear rupture produces in the ground a seismic shock wave similar to the sonic boom produced by a supersonic airplane. This shock wave may increase the destruction caused by the earthquake. We report that supershear earthquakes are characterized by a specific pattern of aftershocks: The fault plane itself is remarkably quiet whereas aftershocks cluster off the fault, on secondary structures that are activated by the supershear rupture. The post-earthquake quiescence of the fault shows that friction is relatively uniform over supershear segments, whereas the activation of off-fault structures is explained by the shock wave radiation, which produces high stresses over a wide zone surrounding the fault.

Although supershear rupture was theoretically predicted more than 30 years ago (*1*–*3*) and first reported over two decades ago (*4*), the realization that it may be common during earthquakes has come only in the past few years (*5*–*13*). This phenomenon can occur only in mode II rupture; that is, when the fault slips in the direction in which rupture propagates. This is the mode of rupture prevalent in large crustal earthquakes. When a fault breaks at supershear speed, the earthquake ground motion is considerably modified (*14*, *15*). We report here that all the faults on which supershear rupture has been inferred have in common a specific pattern of aftershocks: The fault itself is remarkably free of aftershocks, which cluster off the fault on secondary structures that are activated by the supershear rupture.

The 1999 moment magnitude (M_w) = 7.4 Izmit earthquake ruptured about 150 km of the North Anatolian fault (NAF) in Turkey. Rupture began near the middle of the fault (Fig. 1) and propagated eastward at supershear speed for about 50 km before decelerating to sub-Rayleigh velocity (*6*). To the west of the epicenter, where the fault broke at classical sub-Rayleigh velocity, the aftershocks defined an E-W linear band that followed the fault under Izmit Bay and the eastern Marmara Sea (Fig. 1 and fig. S2A), except for two aftershock clusters located near the termination of the fault and associated with geothermal activity and branching (*16*, *17*).

To the east of the epicenter, the aftershock pattern was different. All along the supershear segment, few aftershocks occurred near the fault trace itself. Instead, they were spread over a broad area surrounding the fault (Fig. 1 and fig. S2B). Between Izmit and Sapanca, the aftershock clusters displayed a NE-SW trend. This orientation follows the lineaments of the old faulting system that characterized the deformation of the region before the development of the NAF (*18*). The aftershock pattern shows that some of these paleofaults, previously thought to be inactive, were partly reactivated by the earthquake. Farther east, between Sapanca and Akyazi, the aftershocks occurred to the south of the rupture on the complex fault system produced by the splaying of the two branches of the NAF. This system consists of a series of short normal faults, bounded to the south and east by strike-slip faults (Fig. 1) (*18*, *19*). The spreading of the aftershocks over the whole area, confirmed by focal mechanisms (*20*), indicates that the whole fault system was activated by the earthquake. The quiescence of the rupture plane itself, which bounds this area to the north, is striking, particularly when one considers that it was the region of highest slip (*21*). Seismic activity reached its peak just beyond the termination of the supershear segment. Farther east, the fault system becomes simpler and, like in the west, aftershocks formed a relatively narrow band parallel to the rupture trace of the slightly north-dipping Karadere segment.

The 1999 M_w = 7.2 Düzce earthquake occurred 3 months after the Izmit earthquake and extended the 150-km-long rupture 40 km eastward. Like the Izmit earthquake, it was a bilateral event nucleating near the middle of the fault (Fig. 2), and near-field recordings show that while rupture propagated westward from the hypocenter at sub-Rayleigh velocity, the average eastward velocity was supershear (*6*, *22*). Aftershocks occurred to the north of the surface rupture, as expected because, unlike the quasi-vertical Izmit rupture, the E-W striking Düzce fault dips about 65° northward (*22*). To the west of the epicenter, except along the fringe of the rupture trace (which corresponds to the shallow part of the fault), aftershocks were distributed rather evenly over the fault plane for a distance of

[1]Centre National de la Recherche Scientifique et Université Joseph Fourier, Grenoble, Laboratoire de Géophysique Interne et Tectonophysique, Boîte Postale 53, 38041 Grenoble, France. [2]Kandilli Observatory and Earthquake Research Institute, Bogaziçi University, Istanbul Kandilli Observatory, 81220 Cengelköy, Istanbul.

*To whom correspondence should be addressed. E-mail: Michel.Bouchon@ujf-grenoble.fr

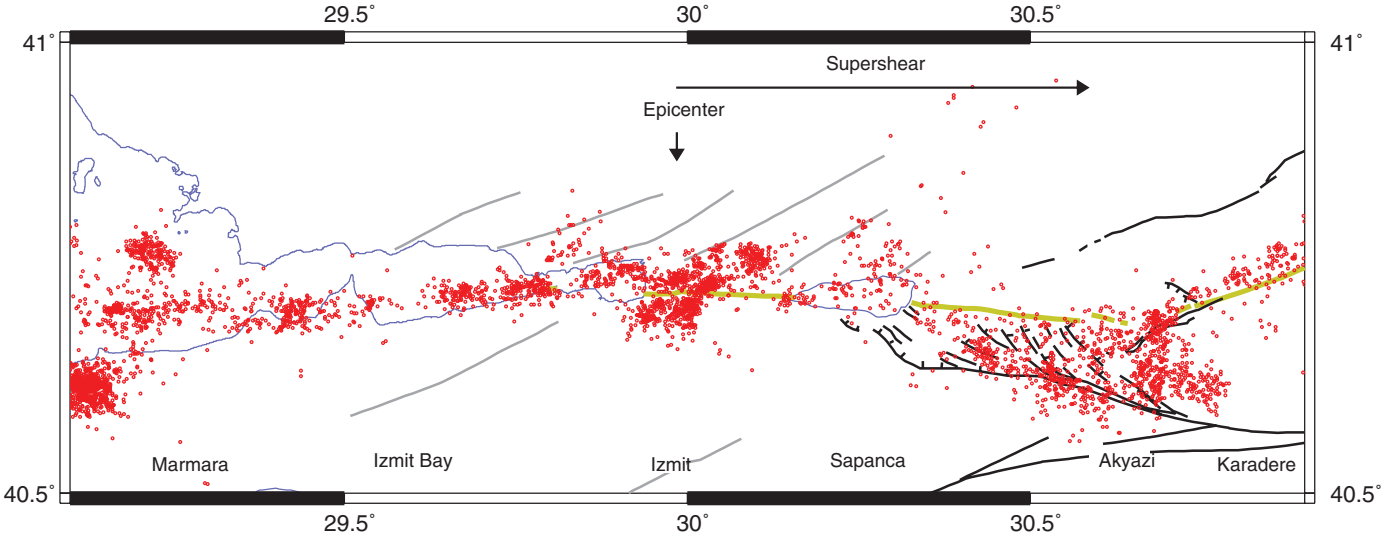

Fig. 1. Map of Izmit aftershocks (red dots) for the period from 17 August to 12 November 1999, relocated after combining all the available data recorded in the region (fig. S1). The surface rupture is in yellow, the active faults in black, and the ones thought to be inactive in gray (*19*).

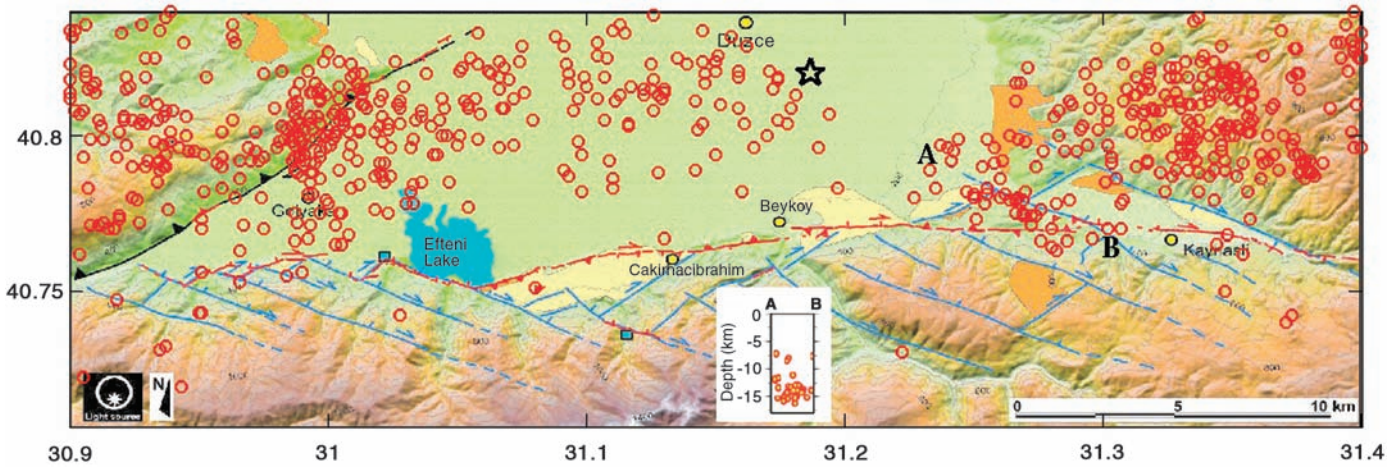

Fig. 2. Map of the Düzce aftershocks (red circles). The epicenters (*37*) are drawn on a background tectonic map (*23*) showing the surface rupture (red) and the plioquaternary fault system (blue). The main shock epicenter is shown by a star. The inset in the middle is the vertical cross-section between A and B.

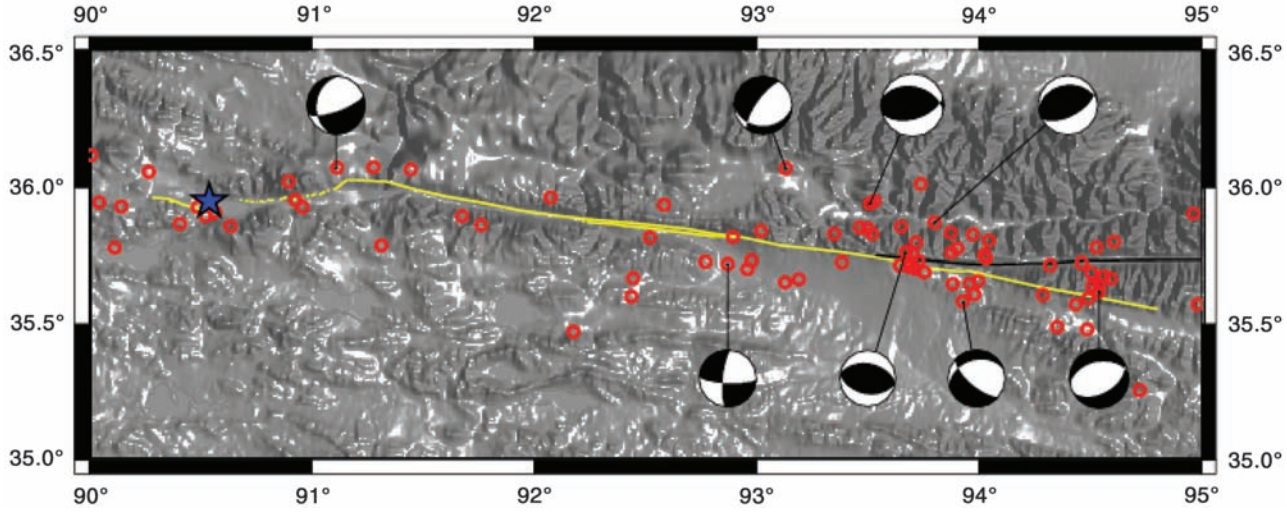

Fig. 3. Map of the Kunlunshan aftershocks of magnitude 4 and higher (red circles), with the focal mechanisms of the largest ones (balloons). The surface rupture is in yellow and the unbroken segment of the Kunlun fault in black. The epicenter is shown by a star.

about 15 km. Beyond this distance, which corresponds to a sharp drop in surface slip (*23*), the density of aftershocks increased, probably reflecting the complex mechanical interaction between the diverging Düzce and Karadere faults in this area.

To the east of the epicenter, the aftershock pattern was notably different. For about 5 km eastward from the hypocenter, the rupture plane was free of aftershocks. Beyond this gap, some aftershock epicenters clustered near the surface trace of the rupture. A cross-section of this cluster (Fig. 2, inset), however, shows that these events occurred at depth and not on the Düzce fault, which is shallow in this area. This WNW-ESE–trending cluster paralleled the old fault system that prevailed in the region before the development of the Düzce fault (*23*) and indicates that the earthquake reactivated some of these paleofaults. Farther east, the number of aftershocks increased near and beyond the termination of the surface break. This area also corresponds to the eastern termination of the mapped trace of the Düzce fault. Beyond it lies the complex 15-km-wide zone of deformation that separates the Düzce fault from the eastern single trace of the NAF.

The 2001 M_w = 7.9 Kunlunshan (Tibet) earthquake produced the longest surface rupture ever observed (Fig. 3), a nearly continuous break extending for about 425 km (*24*). Most of the rupture—about 300 km—occurred at supershear speed (*7*, *10*). In spite of its large magnitude, the earthquake was followed by few aftershocks (*10*, *25*). The strongest one reached a M_w of only 5.6, much lower than the value of about 6.8 typically expected for an event of this size. Only 17 aftershocks had a body wave magnitude m_b of 5 or higher, whereas on average for the magnitude of the main shock, more than 70 could have been expected (*26*). Another unusual feature of the Kunlunshan sequence is that out of the eight largest aftershocks for which focal mechanism could be determined (*27*, *28*), only one event of relatively small magnitude (M_w = 5.1) had a mechanism similar to that of the main shock (Fig. 3). Although the absence of local stations prevents precise locations, this is a strong indication that most of the aftershocks occurred not on the rupture plane, but on secondary structures off the main fault. The fact that the longest surface rupture ever observed was directly the source of so few aftershocks of such small magnitude is astonishing. Seismic activity, although small, clustered in two areas: the mechanically complex zone where the rupture splayed off the main Kunlun fault and the near-termination of the surface rupture. Thus, like at Izmit and Düzce, the long supershear segment of the Kunlunshan earthquake was quiet. The small aftershock activity of the region was concentrated near the junction of the rupture plane with other faults and near the termination of the supershear rupture.

The 2002 M_w = 7.9 Denali fault (Alaska) earthquake produced a surface rupture of about 340 km. Rupture started on a 48-km-long north-dipping thrust fault, the Sustina Glacier fault, then propagated eastward for nearly 300 km as a

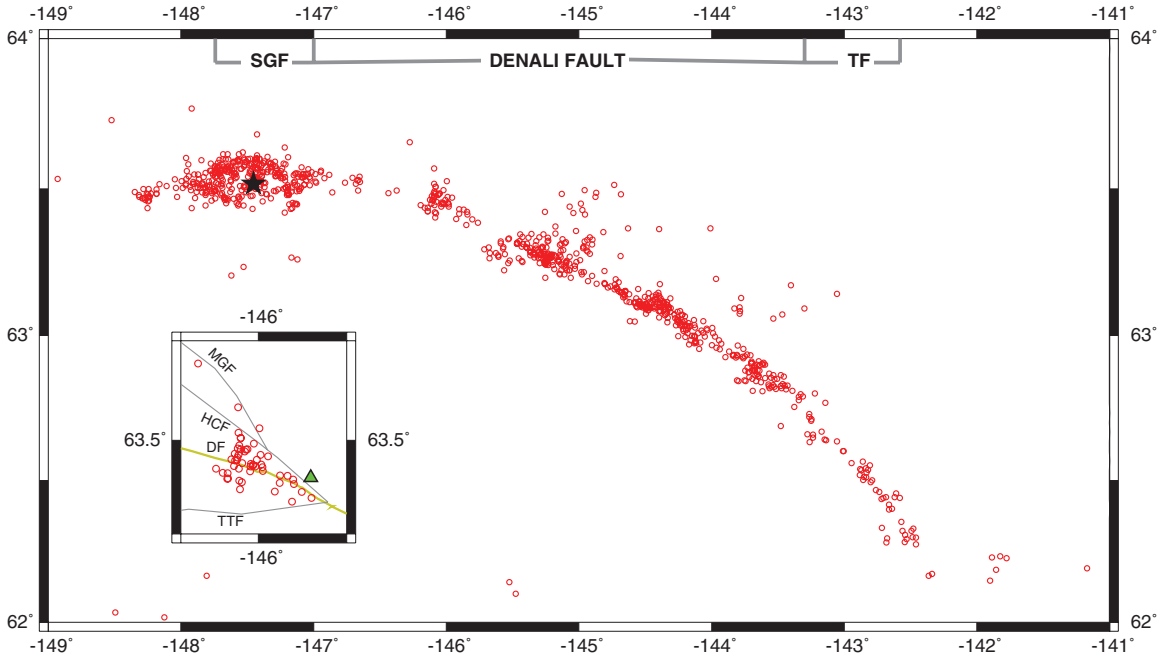

Fig. 4. Map of the Denali aftershocks of magnitude 3 and higher (red circles). The epicenter is shown by a star (SGF, Sustina Glacier fault; TF, Totschunda fault). The inset is a zoom of the 146° cluster, with the surface rupture in yellow and the fault nest in gray (MGF, McGinnis Glacier fault; HCF, Hines Creek fault; DF, Denali fault; TTF, Talkeetna fault). The accelerometer location is indicated by a triangle.

strike-slip rupture along the adjacent Denali and Totschunda faults (*29*). The length of the supershear segment is not precisely known, but modeling of the lone near-fault accelerometer records suggests that the supershear episode began about 35 km before the accelerometer site (*9*), at a longitude of about 146.5° (Fig. 4). A supershear speed of 5.5 km/s (*8*, *9*) and an average rupture velocity of 3.3 km/s (*30*) yield an estimate of about 60 km for the length of the supershear segment.

Aftershocks were distributed (Fig. 4) in a nearly continuous band along the 340 km of rupture, with the notable exception of the fault stretch between 146.5° and 145.5°. Except for a cluster of events centered around 146°, this stretch lacked aftershocks. This cluster was associated with a nest of faults (Fig. 4, inset) that merge there with the Denali fault. Geophysical investigations of this area (*31*, *32*) show that the aftershocks clustered on these secondary faults, principally the south-dipping Hines Creek fault and the north-dipping Talkeetna thrust fault, located respectively north and south of the Denali fault. In this zone, the Denali fault is nearly vertical and was almost free of aftershocks (*31*, *32*). Farther east, between 145.5° and 145°, where supershear is inferred to have ended, a broad aftershock cluster was present. There again, geophysical imaging has shown that these aftershocks clustered, not on the vertical Denali fault but on two shallow-dipping secondary faults, the McCallum Creek–State Creek and the Donnelly Dome–Granite Mountain thrust faults located on opposite sites of the Denali fault (*31*). Focal mechanisms of events in this cluster confirm that most of them, including the largest aftershock of the earthquake, had thrust mechanisms (*33*). Along the inferred supershear stretch, few aftershocks are associated with the Denali fault itself. Aftershocks in this zone cluster on well-recognized secondary faults located on both sides of the vertical Denali fault.

The relative quiescence of supershear segments shows that friction (*34*) was more uniform over these segments than elsewhere on the fault. This explains the puzzling low ground accelerations recorded near supershear segments (*6*, *8*), because the high-frequency seismic radiation, which dominates the acceleration spectrum, is controlled by faulting heterogeneities (*35*). The clustering of the aftershock activity on secondary faults located off the rupture plane is also readily explained: The shock wave radiated by the supershear rupture produces high stresses over a wide zone surrounding the fault (*36*). In this area the stress carried on the Mach cone is nearly the same as that which occurs on the fault (*36*). The width of this zone is comparable to the depth of faulting, in agreement with the present observations.

References

1. R. Burridge, *Geophys. J.* **35**, 439 (1973).
2. D. J. Andrews, *J. Geophys. Res.* **81**, 5679 (1976).
3. S. Das, K. Aki, *Geophys. J. R. Astron. Soc.* **50**, 643 (1977).
4. R. J. Archuleta, *J. Geophys. Res.* **89**, 4559 (1984).
5. S. Das, *Science* **317**, 905 (2007).
6. M. Bouchon *et al.*, *Geophys. Res. Lett.* **28**, 2723 (2001).
7. M. Bouchon, M. Vallée, *Science* **301**, 824 (2003).
8. W. L. Ellsworth *et al.*, *Earthquake Spectra* **20**, 597 (2004).
9. E. M. Dunham, R. J. Archuleta, *Bull. Seismol. Soc. Am.* **94**, S256 (2004).
10. D. P. Robinson, C. Brough, S. Das, *J. Geophys. Res.* **111**, B08303 (2006).
11. A. J. Rosakis, O. Samudrala, D. Coker, *Science* **284**, 1337 (1999).
12. K. Xia, A. J. Rosakis, H. Kanamori, J. R. Rice, *Science* **308**, 681 (2005).
13. X. Lu, N. Lapusta, A. J. Rosakis, *Proc. Natl. Acad. Sci. U.S.A.* **104**, 18931 (2007).
14. B. T. Aagaard, T. H. Heaton, *Bull. Seismol. Soc. Am.* **94**, 2064 (2004).
15. P. Bernard, D. Baumont, *Geophys. J. Int.* **162**, 431 (2005).
16. S. Özalaybey *et al.*, *Bull. Seismol. Soc. Am.* **92**, 376 (2002).
17. H. Karabulut *et al.*, *Bull. Seismol. Soc. Am.* **92**, 387 (2002).
18. O. Emre *et al.*, *Mineral Res. Expl. Bull.* **120**, 119 (1998).
19. O. Emre, Y. Awata, in *Surface Rupture Associated with the 17 August 1999 Izmit Earthquake* (General Directorate of Mineral Research and Exploration, Ankara, Turkey, 2003), pp. 31–39.
20. G. Örgülü, M. Aktar, *Geophys. Res. Lett.* **28**, 371 (2001).
21. A. A. Barka *et al.*, *Bull. Seismol. Soc. Am.* **92**, 43 (2002).
22. M. P. Bouin, M. Bouchon, H. Karabulut, M. Aktar, *Geophys. J. Int.* **159**, 207 (2004).
23. S. Pucci, thesis (Universita degli Studi di Perugia, Italy, 2006).
24. Y. Klinger *et al.*, *Bull. Seismol. Soc. Am.* **95**, 1970 (2005).
25. M. Antolik, R. E. Abercrombie, G. Ekström, *Bull. Seismol. Soc. Am.* **94**, 1173 (2004).
26. P. A. Reasenberg, L. M. Jones, *Science* **243**, 1173 (1989).
27. www.globalcmt.org.
28. P. Hao *et al.*, *Acta Seismol. Sinica* **17**, 31 (2004).
29. D. Eberhart-Phillips *et al.*, *Science* **300**, 1113 (2003).
30. D. D. Oglesby *et al.*, *Bull. Seismol. Soc. Am.* **94**, S214 (2004).
31. T. M. Brocher *et al.*, *Bull. Seismol. Soc. Am.* **94**, S85 (2004).
32. M. A. Fisher *et al.*, *Bull. Seismol. Soc. Am.* **94**, S107 (2004).
33. N. A. Ratchkovski, S. Wiemer, R. A. Hansen, *Bull. Seismol. Soc. Am.* **94**, S156 (2004).
34. R. Madariaga, *Science* **316**, 842 (2007).
35. R. Madariaga, *Ann. Geophys.* **1**, 17 (1983).
36. H. S. Bhat *et al.*, *J. Geophys. Res.* **112**, B06301 (2007).
37. S. Özalaybey *et al.*, paper presented at the 27th General Assembly of the European Seismological Commission, Lisbon, Portugal, 10 September 2000.

Supporting Online Material

www.sciencemag.org/cgi/content/full/320/5881/1323/DC1
SOM Text
Figs. S1 and S2
References

9 January 2008; accepted 5 May 2008
10.1126/science.1155030